PERGAMON

European Journal of Cancer 36 (2000) 1876–1884

European Journal of Cancer

www.ejconline.com

Regulation of tumour drug delivery by blood flow chronobiology

R.D. Blumenthal [a,*], L. Osorio [a], R. Ochakovskaya [a], Z. Ying [b], D.M. Goldenberg [a]

[a] *Garden State Cancer Center, 520 Belleville Avenue, Belleville, NJ 07109, USA*
[b] *Department of Statistics, Rutgers University, Piscataway, NJ 08859, USA*

Received 17 December 1999; received in revised form 30 March 2000; accepted 3 April 2000

Abstract

The chronobiology of various physiological phenomena that impact tumour drug delivery has not been established. Since the delivery of therapeutic agents is directly influenced in part by tumour vascular volume (VV), vascular permeability (VP) and local blood flow (BF), we have performed a series of studies to assess the natural rhythms of these functions in tumour and normal tissues. Preliminary results by Hori *et al. Cancer Res* 1992, **52**, 912–916, have demonstrated fluctuations in tumour blood flow in subcutaneous (s.c.) rat tumours with a higher rate at 15–21 h after light onset (HALO) compared with 3–9 HALO. We used the GW-39 and LS174T human colon carcinoma xenografts grown s.c. in nude mice for these studies. VV, VP and BF were determined at 3, 7, 10, 13, 17, 20 and 23 HALO. In separate studies, dosing with a small therapeutic agent ([^{3}H]-5-fluorouracil (5-FU)) or a macromolecule ([^{131}I]-131-MN-14-anti carcinoembryonic antigen (CEA) immunoglobulin G (IgG)) was done at 10 and 17 HALO and 3, 10 and 17 HALO, respectively, and tissue and tumour uptake was determined in each group. Well-defined peaks and nadirs were observed for all three vascular functions. The peaks for VV and VP were similar in tumour and normal tissue whereas BF rate had a unique rhythm in tumour. Using cosinor analysis of the BF rate, we have found that the acrophase (peak) for tumour BF occurs at approximately 17 HALO in both tumour xenografts, while maximal liver, lung and kidney BF occurred at 10–13 HALO. Tumour BF rate ranged from the lowest value of 1.34±0.54 μl/g/min at 20 HALO to the highest value of 2.79±0.57 μl/g/min at 17 HALO. Liver BF rate ranged from 4.1±1.1 μl/g/min at 3 HALO to 10.22±1.31 μl/g/min at 10 HALO, and was 5.83±1.37 μl/g/min at 17 HALO. Thus, the rhythm of tumour and normal tissue BF are different, creating a window of opportunity when tumours can be targeted with a therapeutic agent. At 3 h postinjection, the %ID/g of 5-FU in tumour at 10 HALO was 0.14±0.09 and at 17 HALO was 0.32±0.12 ($P < 0.02$). In liver at 10 HALO, uptake was 0.13±0.06 and at 17 HALO was 0.07±0.03 ($P < 0.05$). At 24 h postinjection, the %ID/g of [^{131}I]-MN-14 IgG in tumour at 10 HALO was 11.50±1.58 and at 17 HALO was 1.5-fold higher at 16.96±2.35 ($P < 0.001$). In liver at 10 HALO, uptake was 6.47±0.49 and at 17 HALO was 30% lower at 4.48±0.81 ($P < 0.01$). These results suggest that small shifts in the chronobiology of BF in tumour and in normal tissue can have a sizeable impact on the distribution of chemotherapeutics and antibody-based drugs.

Keywords: Author to supply

1. Introduction

In radiotherapy, the efficacy of treatment depends upon the local oxygen concentration that is governed by the local blood flow (BF). Transient reduction in the tumour BF can also be an advantage for the activity of drugs that are more cytotoxic in a hypoxic or acidic environment [1]. In addition, such transient reductions can be used to manipulate drug pharmacokinetics. For example, if the BF were reduced when drug levels in the tumour are maximal, the exposure time of tumour cells to the drug would increase.

In chemotherapy, immunotherapy and gene therapy, blood flow plays an important role in the delivery of appropriate agents [2,3], which in turn influences the efficacy of therapy. Tumours with a greater blood flow and vascular permeability have been shown to be better targeted [4]. Pharmacological modulation of the tumour blood flow further enhances the delivery of drugs to tumours [5]. Since functional differences exist in the microcirculation of normal tissue and tumours, it has

* Corresponding author. Tel.: +1-973-844-7014; fax: +1-973-844-7020.

E-mail address: rblumenthal.gscancer@worldnet.att.net (R.D. Blumenthal).

0959-8049/00/$ - see front matter
PII: S0959-8049(00)00177-5

been possible to use pharmacological agents, like angiotensin II (AT II), to selectively enhance tumour blood flow and thereby increase drug delivery and therapeutic outcome [6]. Similarly, Zhou and colleagues have used propranolol or AT II to increase the uptake of radiolabelled antibody or drug-conjugated antibody, and thus achieved a greater tumour growth inhibition [7]. In another key study, β-adrenergic blocking agents were capable of increasing tumour:blood and tumour: liver delivery of macromolecules, such as ^{125}I-labelled antibody conjugates. These radio- or drug–conjugate-treated mice had smaller tumour sizes and a greater number of regressions than mice that did not receive the β-blocker [8]. However, Pimm has reported that although propranolol and pindolol could increase BF in some tumours, uptake of macromolecules was not increased [9]. In past publications, we have demonstrated that tumour vascular properties affect tumour targeting [10,11]. However, the chronobiology of many physiological phenomena that impact upon tumour targeting with non-specific and specific agents has not yet been established. Preliminary results by Hori and colleagues have demonstrated circadian fluctuations in tumour blood flow in subcutaneous rat tumours, with a 56% higher rate at 15–21 HALO compared with the rate at 3–9 HALO [12].

Circadian rhythms in DNA synthesis of tumour cells have also been reported [13,14]. These results suggest that there might be an optimal time to administer anticancer drugs, since they exert their greatest effects when cells are actively dividing and/or in specific phases of the cell cycle. For example, doxorubicin was shown to be more effective when administered at 16 HALO than at 4 HALO [15]. The time during which tumour blood flow increases (approximately 16 HALO) coincides with the time during which tumour growth becomes more rapid [16].

In this report, we investigate the natural rhythms of vascular permeability (VP), vascular volume (VV) and local blood flow (BF) in tumorous and normal tissues and the effects of these rhythms on accretion of small molecule and micromolecule therapeutics.

2. Methods and materials

2.1. Animal model

Non-tumour-bearing male athymic nude mice from Taconic (Germantown, NY, USA; 5–6 weeks old or with a minimum starting weight of 18 g) were used for these studies. Male mice were selected to avoid the influence of the oestrous cycle on tissue proliferative activity and physiological function. Mice were implanted either with 200 μl of a 10% GW-39 human colonic tumour suspension or 200 μl containing 1×10^7 LS174T human colonic tumours cells grown in culture. GW-39 tumours have been serially propagated in animals since 1966 [17]. LS174T was purchased from ATCC (Rockville, MD, USA) and grown in Roswell Park Memorial Institute (RPMI) 1640 media containing 10% fetal bovine serum, 1% L-glutamine and 1% penicillin-streptomycin. Animal care was provided in accordance with institutional guidelines. Animals were placed in one of three 12:12 light: dark schedules as shown in Fig. 1 for 3 weeks prior to the start of any study to allow for the standardisation of chronobiological rhythms. Room temperature was maintained at 22±2°C.

2.2. Quantitation of vascular volume (VV) and vascular permeability (VP)

VV and VP were normalised to tumour size. VV and VP were quantitated using an *in vivo* labelling method of red blood cells (RBC). Animals were injected intravenously (i.v.) with 2.5 ng stannous chloride (Dupont/NEN Products, N. Billerica, MA, USA), followed 30 min later by an intravenous injection of 15 μCi (0.56

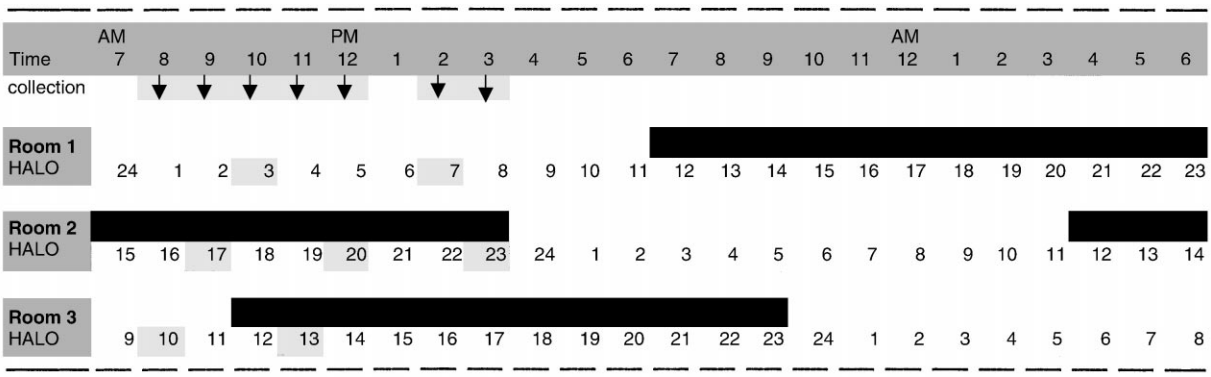

Fig. 1. Animals were placed on one of three 12:12 light:dark schedules as shown for weeks prior to the start of any study to allow for standardisation of chronobiological rhythms. Room temperatures were kept at 22±2°C. Shading around 3, 7, 10, 13, 17, 20 and 23 are the HALO samples. The time collection is the time of day over a 24 h cycle. The black shading indicates when the lights were switched off in each of the three rooms. During HALO 1–12 the lights were on and from 12–24 the lights were off.

MBq) $^{99m}TcO_4$ (Mallinckrodt, St. Louis, MO, USA) and 3 μCi (0.11 MBq) of ^{125}I-labelled irrelevant isotype matched MAb (Ag8). One hour later, the animals were anaesthetised and bled by intracardiac puncture. The animals were killed by cervical dislocation and the tissues were removed, weighed and counted with a gamma scintillation counter. VV and VP were calculated using the following formulas [10,17]:

$$\mathrm{VV} = \mu\mathrm{l\ blood/g\ tissue}$$

$$= \left(^{99m}\mathrm{Tc/g\ tissue}\right)/\left(^{99m}\mathrm{Tc/g\ blood}\right) \times 1000;$$

$$\mathrm{VP} = \text{total plasma in tissue} - \text{intravascular plasma}$$

$$= \left[\left(^{125}\mathrm{I/g\ tumour}\right)/\left(^{125}\mathrm{I/g\ plasma}\right)\right] - [\mathrm{VV} \times (1\text{-haematocrit})].$$

2.2.1. Blood flow measurements

BF was calculated by measuring [^{86}Rb]- uptake [18] as first used by Saperstein [19]. The animals were killed 1 min after caudal injection of 5 μCi of [^{86}Rb]. The tissues were collected, weighed and counted. The per cent injected dose per gram (%ID/g) within 1 min after i.v. injection is analogous to the tissue vascular perfusion as a percentage of cardiac output per gram. The following formula was used to calculate BF (μl/g/min) = per cent injected dose/gram × total blood volume (TBV = 1.2 ml for a mouse). For GW-39, 10 mice per HALO were used and for LS174T tumours, five mice per HALO were used. The average±standard deviation (S.D.) for each group is presented. The two-sample *t*-test was used to test the difference of two vascular values. Critical values of the T-distribution for a two-tailed test were obtained from J.H. Zar [20].

2.2.2. Cosinor analysis

In studies that have 7 HALO points, points were fit to a 24 h cosine by the method of least squares [21,22] and cosinor analysis was used to find the best-fit cosine curve. These curves allowed us to determine the acrophase (time of highest value) mesor (rhythm-adjusted mean value) and amplitude (half of the peak–trough difference). Results of cosinor analysis were used to compare acrophases of cosinor curves specifically, since estimates of acrophases were approximately normally distributed and standard error estimates were available from the cosinor analysis [22].

2.3. Radioantibody preparation

MN-14 anticarcinoembryonic antigen (CEA [23]) for accretion studies and non-specific Ag8 for VP studies were radioiodinated by the chloramine-T method [23]. Free radioiodine was removed from the product by size exclusion over a PD-10 column (Pharmacia, Piscataway, NJ, USA) equilibrated with 0.04 M phosphate-buffered saline (0.04 M phosphate, 0.15 M NaCl, 0.02% NaN_3), pH 7.4, containing 1% human serum albumin. Routine quality assurance of the radioiodinated antibody was performed by size-exclusion high performance liquid chromatography (HPLC) using Zorbax GF-250 (Dupont, Wilmington, DE, USA) columns to ensure $<5\%$ aggregation and $<4\%$ free radioiodine.

2.4. Tumour accretion studies

To determine the uptake of a particular agent in the tumour and normal tissues as a function of different BF rates (different HALOs), separate groups of animals bearing size-matched, s.c. tumours were injected i.v. with 30 μCi of [^{3}H]-5-fluorouracil (5-FU) and 10–15 μCi of the agent of interest. Uptake was monitored 3 h post 5-FU and at 24 h post radioantibody and six mice per time point were used. At the time of sacrifice, mice were given sodium pentobarbital, bled by cardiac puncture, and then killed by cervical dislocation. Tumours and organs (liver, kidney, lung) were excised, weighed and counted in a scintillation counter using appropriate windows for [^{131}I]. Samples were then stored frozen for 11 half lives (90+ days) for radioiodine decay and then recounted in a β-counter for [^{3}H]. Counts per minute (CPM) per tissue were normalised to tissue weight and for total CPM injected and recorded as the per cent injected dose per gram (%ID/g). Differences in accretion at 10 and 17 HALO for 5-FU and at 3, 10 and 17 HALO for [^{131}I]-immunoglobulin G (IgG) were evaluated by a two-tailed *t*-test. The test measures the probability that differences between treatment groups could occur by chance alone. A P value of <0.05 was considered significant.

3. Results

3.1. Chronobiology of vasopermeability

We have used the method of Sands and Gallagher to measure vascular volume (VV; Tc99m-RBCs) and vascular permeability (VP; [^{125}I]-IgG) in GW-39 s.c. nude mice. A fixed periodicity (Fig. 2) for VV with a peak at 23 HALO (6 a.m.) of 80.5±15.9 μl/g and secondary peaks at 17 and 13 HALO (12 a.m. and 8 p.m.) of 62.4±11.7 and 57.4±4.6 μl/g, respectively, was observed for the tumour. VV for the remaining four time-points was under 14 μl/g ($P<0.001$ compared with 13, 17 and 23 HALO). Peak times of VV were similar for liver, lung and kidney, although the variability between the seven points was much less in kidney (range of 48.8±15.2 μl/g at 20 HALO to 106.2±12.8 μl/g at 23 HALO). Fluctuations in tumour VP (Fig. 3) also exist, with the average peak VP occurring at 17 HALO

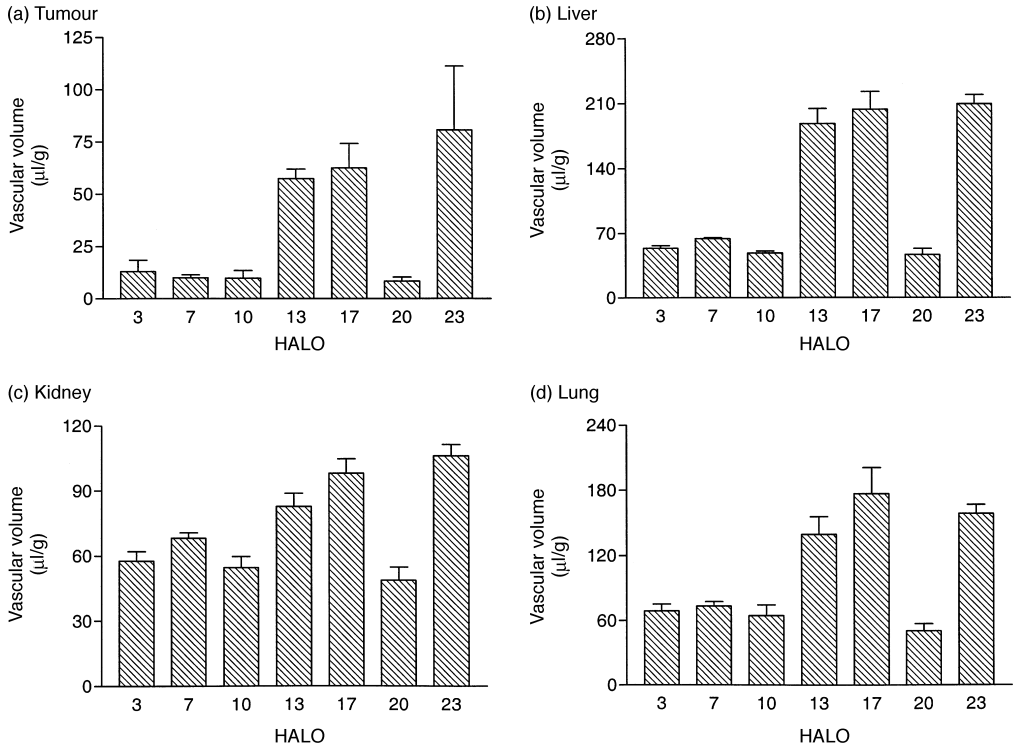

Fig. 2. Using the method of Sands and Gallagher, vascular volume (VV; Tc99m-red blood cells (RBCs)) was determined at each of 7 h after light onset (HALOs) in GW-39 subcutaneous (s.c.) nude mice (average of $n=6$ per HALO recorded).

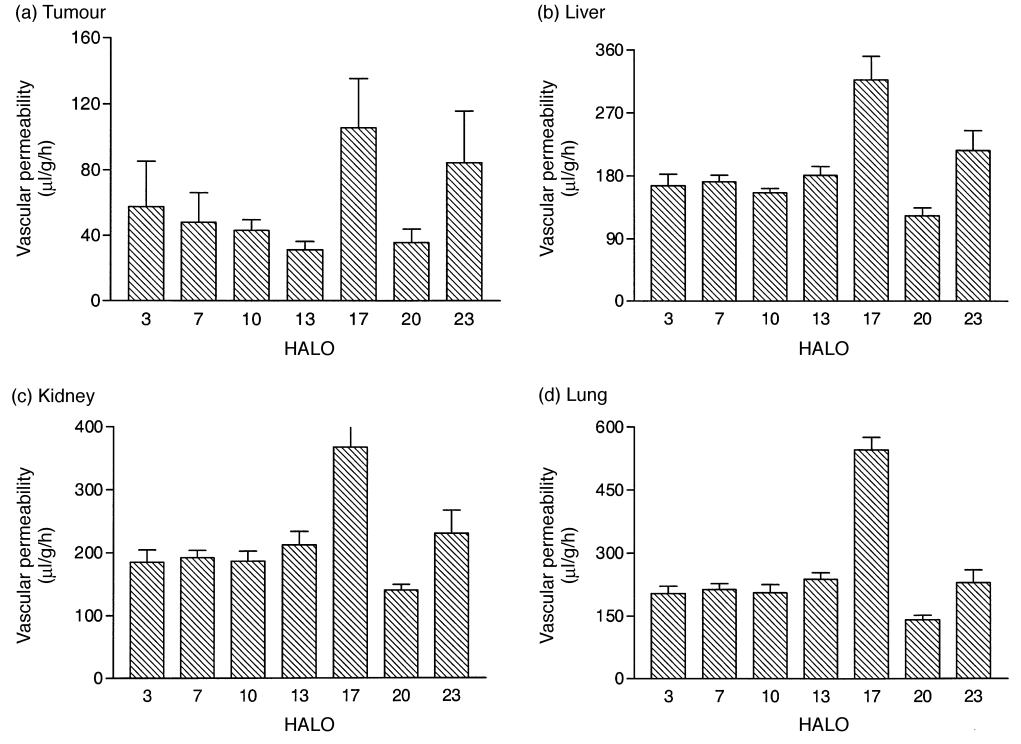

Fig. 3. Using the method of Sands and Gallagher, vascular permeability (VP; [^{125}I]-IgG) was determined at each of 7 h after light onset (HALOs) in GW-39 subcutaneous (s.c.) nude mice (average of $n=6$ per HALO recorded).

(105.7±29.6 µl/g/h) and at 23 HALO (84.5±31.1 µl/g/h). Although there is a VV peak at 13 HALO, VP is at its lowest at that time (31.2±5.2 µl/g/h). The time for peak and nadir VP in normal liver and lung was identical to the tumour. The kidney profile was similar, although the amplitude was not as great as for liver, lung or

tumour, with the exception of a peak at 17 and a trough at 20 HALO. This perhaps reflects the unique role of kidney; i.e. continuous exchange of material between capillaries and nephron tubules. These results suggest that the mechanism(s) regulating the natural rhythm of VP (e.g. vascular endothelial growth factor (VEGF) production) is not unique to tumours. However, it highlights a preferred time of day when macromolecules are more likely to permeate blood vessels, which may provide a window of opportunity for dosing, in particular, when delivering a tumour-specific agent such as an antibody.

3.2. Chronobiology of blood flow

GW-39 BF in the tumour ranged from the lowest value of 1.34±0.54 μl/g/min at 20 HALO (3 a.m.) to the highest value of 2.79±0.57 μl/g/min at 17 HALO (12 a.m.; $P<0.01$; Fig. 4). The differences between time points could not be accounted for by differences in the blood clearance of ^{86}Rb, since blood values were similar at each time-point measured (data not shown). Cosinor analysis of the tumour data shows that the mesor is 1.924 and the amplitude is 0.369 (Table 1). The acrophase occurs at 232 degrees. Curve fitting thus indicates that for the GW-39 tumour, the highest point occurs at 10.47 p.m. and the lowest point occurs at 6.27 p.m. In contrast, normal tissue BF peaked at 10–13 HALO. For example, liver BF peaked at 10.22±1.31 μl/g/min at 10 HALO (5 p.m.) and was only 5.83±1.37 μl/g/min at 17 HALO ($P<0.001$). Cosinor analysis of liver data showed an acrophase of 182 degrees or 12.13 HALO and the lowest point occurring at 0.13 HALO. Similarly, lung BF peaked at 10 HALO (5 p.m.) with a value of 16.70±5.09 μl/g/min and was lowest at 20–23 HALO (10.26±0.95; $P<0.02$) and kidney also had the highest BF at 10 HALO (60.35±10.06 μl/g/min) and the lowest at 20–23 HALO (35.6±4.51; $P<0.001$). These results suggest that the regulation of tumour BF at any particular time of day is different from the regulation of BF in normal tissue. It may also be possible to take advantage of the discrepancy in time of peak BF to dose when BF is maximal for tumour and less than maximal for normal tissue to deliver higher and more efficacious doses of cytotoxic therapy.

Using a second human colonic xenograft model (LS174T tumours implanted s.c. in nude mice), the BF rate was calculated at the same seven HALO points. As shown in Fig. 4, the acrophase for liver BF was at 11 HALO (5:00 p.m.) and for tumour BF was 15.5 HALO (10:30 p.m.; $P=0.056$), suggesting that regulation of tumour BF is similar in different tumour xenografts and that normal tissue BF regulation is distinct from tumour regulation.

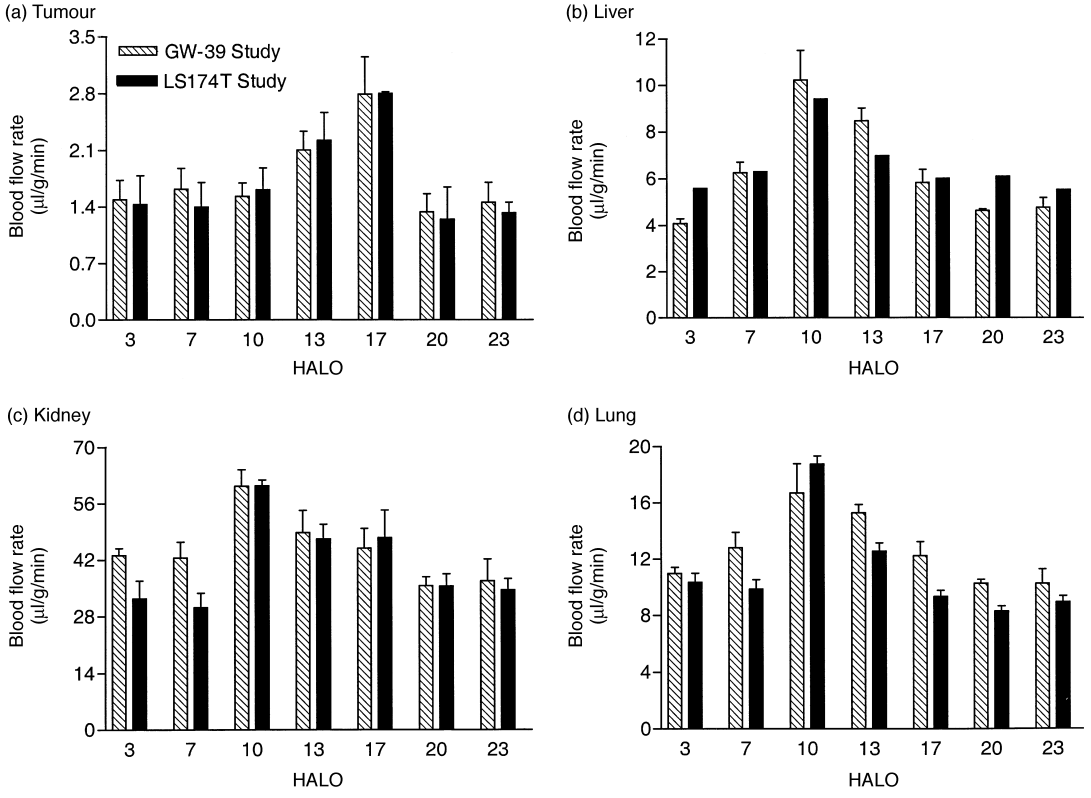

Fig. 4. Blood flow (BF) rate ([^{86}Rb] distribution) was determined in mice bearing GW-39 or LS174T colon tumours — two studies each with five mice per time-point ($n=10$ total) for GW-39 subcutaneous (s.c.) tumours and one study with five mice per time-point for LS174T s.c. tumours by the [^{86}Rb] tracer method. The mean at each time-point is recorded.

Table 1
Cosinor analysis of blood flow (BF) rate rhythm

	Tumour	Liver
Mesor	1.924	2.988
Amplitude	0.369	3.176
Acrophase	232° (15.47 h)	182° (12.13 h)
Low point	11.27 h	0.13 h

In the final studies, the effect of circadian blood flow differences on accretion of small and large molecular weight therapeutic agents was determined. We assessed the uptake of [^{3}H]-5-FU (<1 K) and [^{131}I]-anti-CEA IgG (150 K) into tumour and normal tissues of GW-39 tumour-bearing nude mice. Fig. 5 (a) shows that at 3 h postinjection, the %ID/g of 5-FU in tumour at 10 HALO was 0.14±0.09 and at 17 HALO was 2.3-fold higher at 0.32±0.12 ($n=6$ per group; $P<0.02$). In contrast, in the liver at 10 HALO, uptake was 0.13±0.06 and at 17 HALO was 1.9-fold lower at 0.07±0.03 ($P<0.05$). Kidney and lung accretion of 5-FU were also significantly higher with a 10 HALO dosing compared with the 17 HALO dosing. Fig. 5 (b) depicts results for macromolecular IgG distribution. At 24 h postinjection, the %ID/g of ^{131}I-MN-14 IgG in tumour when dosed at 10 HALO was 11.50±1.58 and when dosed at 17 HALO was 1.5-fold higher at 16.96±2.35 ($n=6$ per group; $P<0.001$). In contrast, in the liver uptake was 6.47±0.49 for a 10 HALO dose and was 30% lower at 4.48±0.81 for the 17 HALO dose ($P<0.01$). The accretion for a 3 HALO dose was similar in tumour to the 10 HALO and for other tissues to the 17 HALO dose (data not shown). The tumour/normal tissue uptake ratios are presented in Table 2. Ratios (tumour:normal tissue) for 5-FU accretion are 12–24-fold higher at 17 HALO compared with those doses at 10 HALO. These effects are not accounted for by differences in blood levels at 10 and 17 HALO since the tumour:blood ratio is only 3-fold at 17 HALO compared with 10 HALO. Ratios for IgG uptake were 1.6–2.3-fold higher with a 17 HALO dosing, compared with results at the 3 and 10 HALO dosing. These results suggest that small shifts in the chronobiology of BF in tumour and in normal tissue can have a sizeable impact on the distribution of chemotherapeutics and antibody-based drugs.

4. Discussion

The studies presented are the first to show detailed fluctuations in the VV, VP and BF rate of tumour and normal tissue blood vessels as a function of the light: dark cycle. The striking changes in each vascular parameter as a function of the time of day imply that when comparing vascular function between different tumours [4,10,24] or between one tumour growing at different sites [11], it is important to make the assessment at the same time of day. The lack of a constant value during a 24-h period for a given function suggests that the mechanism regulating each function is influenced by some built-in circadian rhythm.

The regulation of tumour blood vessel structure and function is an active area of investigation [25]. Chronomodulation of vascular function represents a new level of exploration of these physiological phenomena, which can readily be linked with the current dogma. For example, present knowledge supports the primary role of VEGF at regulating vessel permeability. Many human tumours synthesise and secrete high levels of VEGF, which is both mitogenic for endothelial cells and stimulates microvascular permeability [26]. Tumours that secrete more VEGF exhibit higher *in vivo* vessel permeability and greater accumulation of drugs [27]. Two high-affinity VEGF receptors (flt-1 and KDR) have been identified on endothelial cells [28,29]. Both VEGF receptors are also upregulated in the endothelial

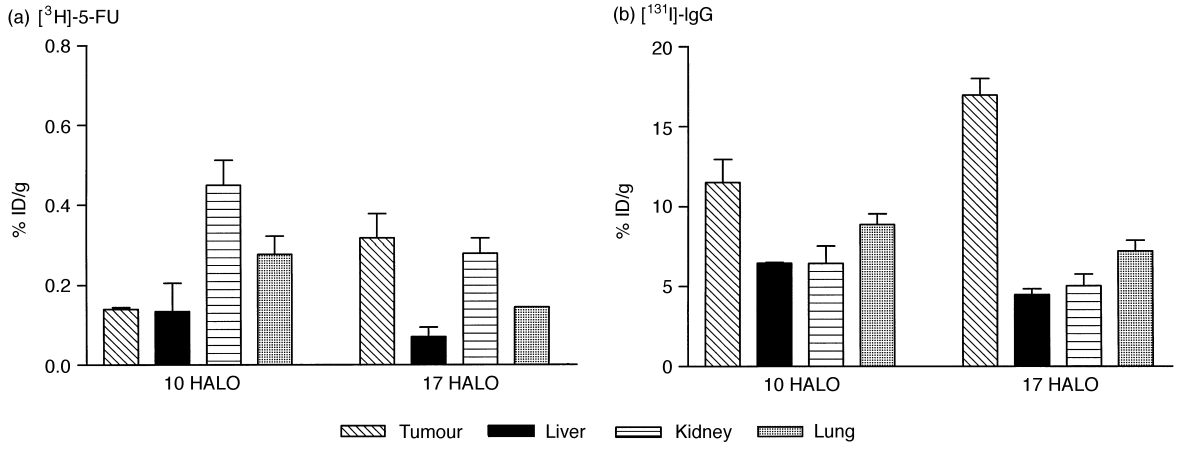

Fig. 5. Uptake (per cent injected dose per gram; (%ID/g)) of (a) [^{3}H]-5-FU at 3 h postinjection and (b) [^{131}I]-IgG at 24 h postinjection in GW-39 tumour-bearing nude mice. The average of six mice at each hour after light onset (HALO) point was recorded.

Table 2
Tumour:non-tumour ratios at various HALOs of dosing

	[^{3}H]-5-FU		[^{131}I]-IgG		
	10 HALO	17 HALO	3 HALO	10 HALO	17 HALO
Tumour/liver	0.37	4.46	2.30	1.77	3.79
Tumour/kidney	0.07	1.13	2.09	1.78	3.37
Tumour/lung	0.13	3.17	1.40	1.29	2.98
Tumour/blood	0.62	1.85	0.75	0.68	1.28

HALO, hours after light onset.

(EC) lining of tumour vasculature, compared with surrounding normal vessels [30,31]. Therefore, changes in the expression of VEGF and/or its receptors may account for the striking differences in VP as a function of HALO. Another downstream factor that regulates tumour vessel permeability is nitric oxide (NO). A change in expression of the enzyme NO synthase (NOS) would alter the amount of NO available and thus alter VP. Many tumour lines have recently also been shown to produce a diverse amount of NOS [32]. Therefore, determining if a periodicity exists for NOS and VEGF expression may also help elucidate the mechanism governing fluctuating VP in both tumour and normal tissue.

Several striking observations can be found in the reported studies. First, the peaks and nadirs for VV and VP are the same for tumour and for normal tissues, while the BF rate peaks at a later time of day than does the normal tissue BF rate. This observation on BF is consistent with the study reported by Hori on fluctuations in tumour blood flow in s.c. rat tumours, which demonstrated a higher rate at 15–21 HALO compared with 3–9 HALO [12]. The overlapping peaks for VP in tumour and non-tumour tissue can still afford an advantage in targeting, in particular, when using an antibody-based therapeutic approach that binds a tumour-associated antigen. Another important finding is that the times for maximum VV and VP and BF in the tumour do not completely overlap with each other. Although 17 HALO is a peak time for all three vascular parameters, unique regulatory mechanisms exist for each vascular function.

Blood flow rate is an important factor regulating drug delivery to tumours and therapeutic outcome. Therefore, the possibility of influencing the distribution of drugs to tumours by administering vasoactive agents is of clinical interest. These agents can increase or decrease vascular resistance to flow by altering tumour vascular diameter (vascular tone; [9]). There are two general approaches taken to selectively affect tumour BF. In the first approach, normal tissues distant from the tumour are actively vasodilated or vasoconstricted with minimal effects on tumour vasculature, but sufficient to induce changes in systemic arterial blood pressure (BP). BF to the tumour would then be governed by changes in perfusion pressure secondary to changes in systemic BP [33]. In the second approach, the normal tissue vascular bed in which the tumour is growing is actively vasodilated or vasoconstricted with minimal effects on the tumour vasculature. The parallel arrangement of the vasculature in the two beds would result in the flow of blood away from the tumour if the normal tissue vasodilates and towards the tumour if the normal tissue vasoconstricts. Numerous papers have reported on the effect of short-term modulation of tumour BF such as noradrenaline, angiotensin (AT II), hydralazine and dexamethasone [34–37]. Studies with the potent vasopressor, AT II, consistently show that after systemic infusion, tumour BF is increased relative to most normal tissues since normal tissue vasoconstricts more readily than tumour tissue [12,38].

The data presented suggest a new concept of BF regulation has emerged related to chronobiology. BF circadian rhythms for the tumour and normal tissue differ, a phenomenon that may be related to the unique structure of the tumour vasculature. The natural BF periodicity in both GW-39 and LS174T tumour xenografts, which is distinct from the rhythm found in normal tissues, provides a window of opportunity for improved tumour:normal tissue targeting of various sized agents. In addition, it raises several questions: (1) What is the nature of the regulation governing the BF rate rhythm in each tissue? (2) Since larger tumours tend to have a lower blood flow than smaller tumours [39], are the chronorhythms for BF similar for small (<0.2 g) and for large tumours (>1.5 g)? (3) Are vaso-modulating agents that affect BF equally effective at different HALOs?

Blood flow rate is directly related to the pressure difference between the arterial and venous ends of the tissue circulation and indirectly related to the resistance to flow. Resistance incorporates many factors, including the effect of blood viscosity, vessel diameter, vessel length and vessel branching. Various methods have been employed to qualitatively and quantitatively assess these parameters in tumour and normal tissues [40,41]. Unlike most normal tissues, the tumour vasculature is highly heterogeneous and does not conform to the standard 'normal' morphology. Its branching pattern is abnormal and chaotic. Tumour vessels also have less smooth muscle and minimal innervation. Therefore,

responses to exogenous and endogenous regulators may differ between tumour and normal tissue. Furthermore, the vascular morphology of one tumour differs from another and to some extent is determined by the growth pattern of the cancer cells [42]. Although the tumour microcirculation originates from the pre-existing vascular network of the host, its organisation may be completely different, depending upon the tumour type, its growth rate and its location in the tumour mass. As a result, the structural (e.g. diameter, surface area) and functional properties (e.g. blood flow, permeability) and responses to pharmacological manipulation may vary between different tumours and will probably differ from normal tissue vessels.

Blood flow is sensitive to changes in pressure difference. Recently, Li and colleagues reported on the rhythmic fluctuations in blood pressure (BP) in mice [43]. Peak BP occurred in the early and late dark period (12–14 HALO and 22–24 HALO). BP was at a minimum in the middle of the light period (7–8 HALO). If BP plays a major role in the changes in tumour BF, then one would expect to see higher tumour BF during the dark cycle. The data in Fig. 4, showing peak tumour BF at 13–17 HALO, partially support this expectation. The drop in BF at 20–23 HALO in spite of high BP is not consistent. However, other factors beside BP may play a role in tumour BF.

Based on BF periodicity data, 17 HALO is the optimal time of dosing with small molecular weight therapeutic agents like 5-FU. This rhythm works well with the rhythm of the enzyme activity metabolising 5-FU. The activity of the enzyme dihydrouracil-dehydrogenase (DHUDase; 1.3.1.2), which results in catabolism of 5-fluoropyrimidines, has a peak at 3 HALO and a trough at 15 HALO [44,45], thus coupling increased tumour delivery with decreased drug metabolism. The peak in BF rhythm also coincides with the optimal time to administer many standard chemotherapeutic agents (e.g. doxorubicin, cisplatin, methotrexate, 5-FU, mitomycin C) based on rhythms in toxicity [46].

Even though tumour accretion of macromolecules like IgGs is a slow process requiring 48–72 h to reach maximal levels, 7-h differences in the time of dosing can result in significant differences in uptake 24 h later. In a separate study, we have found that haematopoietic toxicity was less when radioantibody was administered later in the day [47]. It may therefore be possible to dose with radioantibody at a time when accretion is maximal based on BF rate, and toxicity is minimal, thus magnifying the therapeutic window.

Application of these types of observations from mice to men can be somewhat difficult, since it is not as easy to control the environment of patients, as it is for laboratory animals. The significant interpatient variability in circadian patterns is a real limitation. However, it may be possible to define specific patient rhythms based on serum levels of certain markers (e.g. cortisol, melatonin and select cytokines). Another concern is that clinically, vascular blood flow is dependent on patient performance status, co-existing disease states and the effects of various medications. Further studies are required to determine whether defined individual tumour BF rhythms exist and can be used towards a therapeutic advantage while taking into account the person's unique physiology and pathology.

In summary, we have demonstrated well-defined fluctuations in VV, VP and BF rates both in tumour xenografts and in three normal tissues. Although the patterns for VV and VP are similar for tumour and non-tumour tissue, the periodicity of the BF rate differs between tumour and normal tissue, thereby resulting in an optimal time to dose that would maximise the tumour:non-tumour ratios. Such phenomena need to be taken into consideration when comparing drug targeting studies in laboratory animals.

Acknowledgements

Supported in part by USPHS grants CA60764 and CA39841 from the NIH.

References

1. Skarsgard LD, Vinczan A, Skwarchuk MW, Chaplin DJ. The effect of low pH and hypoxia on the cytotoxic effects of SR4233 and mitomycin C in vitro. *Int J Radiat Oncol Biol Phys* 1994, **29**, 363–367.
2. Jain RK. Determinants of tumor blood flow: a review. *Cancer Res* 1988, **48**, 2641–2658.
3. Chaplin DJ, Hill SA, Bell KM, Tozer GM. Modification of tumor blood flow: current status and future directions. *Semin Radiat Oncol* 1998, **8**, 151–163.
4. Sands H, Jones P, Shah S, Palme D, Vessella R, Gallagher B. Correlation of vascular permeability and blood flow with monoclonal antibody uptake by human Clousner and Renal Cell xenografts. *Cancer Res* 1988, **48**, 188–193.
5. Bomber P, McCreedy R, Hambersley P. Propranolol hydrochloride enhancement of tumor perfusion and uptake following gallium-67 in a mouse sarcoma. *J Nucl Med* 1986, **27**, 243–245.
6. Suzuki M, Hori K, Abe I, Saito S, Sato H. A new approach to cancer chemotherapy: selective enhancement of tumor blood flow with angiotensin II. *J Natl Cancer Inst* 1981, **67**, 663–669.
7. Zhou S, Wang N, Liu T, Dong Z. Experimental study of tumor directed therapy with gastric cancer monoclonal antibody–mitomycin conjugate combined with propranolol or angiotensin II. *Acta Pharm Sinica* 1992, **27**, 891–894.
8. Smyth M, Pietersz G, McKenzie I. Use of vasoactive agents to increase tumor perfusion and the antitumor efficacy of drug–monoclonal antibody conjugates. *J Natl Cancer Inst* 1987, **79**, 1367–1373.
9. Pimm M. An examination of the influence of vasoactive drugs on blood flow and localisation of a monoclonal antibody in human tumor xenografts. *Br J Cancer* 1990, **62**, 69–71.
10. Blumenthal RD, Sharkey RM, Kashi R, Natale AM, Goldenberg DM. Physiological factors influencing radioantibody uptake: a

study of four human colonic carcinomas. *Int J Cancer* 1992, **51**, 935–941.
11. Blumenthal RD, Sharkey RM, Kashi R, Natale AM, Goldenberg DM. Influence of animal host and tumor implantation site on radio-antibody uptake in the GW-39 human colonic cancer xenograft. *Int J Cancer* 1989, **44**, 1041–1047.
12. Hori K, Suzuki M, Tanda S, Saito S, Shinozaki M, Zhang Q. Circadian variation of tumor blood flow in rat subcutaneous tumors and its alteration by angiotensin II-indirected hypertension. *Cancer Res* 1992, **52**, 912–916.
13. Smaaland R, Laerum OD, Abrahamsen JF, Sothern RB, Lote K. Cytokinetic circadian patterns in human host and tumor. *J Infus Chemother* 1995, **5**, 11–14.
14. Hrushesky WJ. Cancer chronotherapy: a drug delivery challenge. *Prog Clin Biol Res* 1990, **341**, 1–10.
15. Hori K, Zhang Q, Li H, Saito S, Sato Y. Timing of cancer chemotherapy based on circadian variations in tumor tissue blood flow. *Int J Cancer* 1996, **65**, 360–364.
16. Hori K, Zhang Q, Saito S. Variation of growth rate of a rat tumour during a light–dark cycle: correlation with circadian fluctuations in tumour blood flow. *Br J Cancer* 1995, **71**, 1163–1168.
17. Goldenberg DM, Witte S, Elster K. A new human tumor serially transplantable in the golden hamster. *Transplantation* 1967, **4**, 760–766.
18. Zanelli G, Lucas P, Fowler J. The effect of anesthesia on blood perfusion in transplanted mouse tumors. *Br J Cancer* 1975, **32**, 380–389.
19. Saperstein L. Regional blood flow by fractional distribution of indicators. *Am J Physiol* 1958, **193**, 161–168.
20. Zar J. *One-sample Hypotheses. Biostatistical Analysis*. Englewood Cliffs, NJ, Prentice Hall, Inc, 1974. 86–100
21. Halberg F, Johnson E, Nelson W, Runge W, Sothern R. Autorhythmometry procedures for physioloic self-measurements and their analysis. *Phys Teacher* 1972, **1**, 1–11.
22. Nelson W, Tong Y, Lee J, Halberg F. Methods for cosinor rhythmometry. *Chronobiologica* 1979, **6**, 866.
23. Sharkey RM, Juweid M, Shevitz HJ, *et al*. Evaluation of a CDR-grafted (humanized) anti-carcinoembryonic antigen (CEA) monoclonal antibody in preclinical and clinical studies. *Cancer Res* 1995, **55**, 5935–5945.
24. Blumenthal RD, Sharkey RM, Kashi R, Sides KRS, Goldenberg DM. Changes in tumor vascular permeability in response to experimenal radioimmunothrapy: a comparitive study of 11 xenografts. *Tumor Biol* 1997, **18**, 367–377.
25. Folkman J. How is blood vessel growth regulated in normal and neoplastic tissue? *Cancer Res* 1986, **46**, 467–473.
26. Collins P, Connolly D, Williams T. Characterization of the increase in vascular permeability factor *in vivo*. *Br J Pharmacol* 1993, **109**, 195–199.
27. Roberts W, Hasan T. Tumor secreted vascular permeability factor/vascular endothelial growth factor influences photosensitizer uptake. *Cancer Res* 1993, **53**, 153–157.
28. Terman BI, Dougher-Vermazen M, Carrion ME, *et al*. Identification of the KDR tyrosine kinase as a receptor for vascular endothelial cell growth factor. *Biochem Biophys Res Commun* 1992, **187**, 1579–1586.
29. de Vries C, Escobedo J, Ueno H, Houck K, Ferrara N, Williams L. The fms-like tyrosine kinase, a receptor for vascular endothelial growth factor. *Science* 1992, **255**, 989–991.
30. Yoshiji H, Gomez DE, Shibuya M, Thorgeirsson UP. Expression of vascular endothelial growth factor, its receptor, and other angiogenic factors in human breast cancer. *Cancer Res* 1996, **56**, 2013–2016.
31. Brown LF, Berse B, Jackman RW, *et al*. Increased expression of vascular permeability factor (vascular endothelial growth factor) and its receptors in kidney and bladder carcinomas. *Am J Pathol* 1993, **143**, 1255–1262.
32. Jenkins D, Charles I, Baylis S, Lelchuk R, Radomski M. Human colon cancer cell lines show a diverse pattern of nitric oxide synthase gene expression and nitric oxide generation. *Br J Cancer* 1994, **70**, 847–849.
33. Chan R, Babbs C, Vetter R, Lamar C. Abnormal response to tumor vasculature to vasoactive drugs. *J Natl Cancer Inst* 1984, **72**, 145–150.
34. Mattsson J, Lilja J, Peterson H. Influence of vasoactive drugs on local tumor blood flow. *Eur J Cancer* 1982, **18A**, 677–684.
35. Noguchi S, Miyauchi K, Nishizawa Y, *et al*. Augmentation of anticancer effect with angiotensin II in intraarterial infusion chemotherapy with breast carcinoma. *Cancer* 1988, **62**, 467–473.
36. Braunschweiger P, Schiffer L. Effect of dexamethasone on vascular function in RIF-1 tumors. *Cancer Res* 1986, **46**, 3299–3303.
37. Jirtle R. Cheminal modification of tumor blood flow. *Int J Hyperthermia* 1988, **4**, 355–371.
38. Tozer G, Shaffi K. Modification of tumor blood flow using the hypertensive agents, angiotensin II. *Br J Cancer* 1993, **67**, 981–988.
39. Kallinowski F, Schlenger KH, Kloes M, Stohrer M, Vaupel P. Tumor blood flow: the principal modulator of oxidative and glycolytic metabolism, and of the metabolic micromilieu of human tumor xenografts *in vivo*. *Int J Cancer* 1989, **44**, 266–272.
40. Solesvik O, Rofstad E, Brustad T. Vascular structure of five human malignant melanomas grown in athymic nude mice. *Br J Cancer* 1982, **46**, 557–567.
41. Grunt T, Lametschwandtner A, Staindl O. The vascular pattern of basal cell tumors: light microscopy and scanning electron microscopic study on vascular corrosion casts. *Microvasc Res* 1985, **29**, 371–386.
42. Rubin P, Casarett G. Microcirculation of tumors. I. Anatomy, function and necrosis. *Clin Radiol* 1966, **17**, 220–229.
43. Li P, Sur SH, Mistlberger RE, Morris M. Circadian blood pressure and heart rate rhythms in mice. *Am J Physiol* 1999, **276**, R500.
44. Naguib F, Soong S, el Kouni M. Circadian rhythm of orotate phosphoribosyltransferase, pyrimidine nucleoside phosphorylases and dihydrouracil dehydrogenase in mouse liver. Possible relevance to chemotherapy with 5-fluoropyrimidines. *Biochem Pharmacol* 1993, **45**, 667–673.
45. Harris B, Song R, Soong S, Diasio R. Circadian variation of 5-fluorouracil catabolism in isolated perfused rat liver. *Cancer Res* 1989, **49**, 6610–6614.
46. Levi F. Chronopharmacology and chronotherapy of cancers. *Path Biol* 1996, **44**, 631–644.
47. Blumenthal R, Reising A, Lew W, Dunn R, Ying Z, Goldenberg D. Chronotolerance of experimental radioimmunotherapy: clearance, toxicity and maximal tolerated dose of I-131-anti-CEA IgG as a function of time of day of dosing in a murine model. *Eur J Cancer* 1999, **35**, 815–824.